ELSEVIER

Contents lists available at ScienceDirect

Computational Biology and Chemistry

journal homepage: www.elsevier.com/locate/cbac



Deciphering synergistic interactions between Curcumin, Piperine, and milk proteins using accurate theoretical methods

Madhesh Palanisamy a,b, Gayathri Krishnamoorthy b,bo, Vidya Ravindran a,b,*

ARTICLE INFO

Keywords:
DFT
Molecular Docking
Traditional Medicine
Synergy
FTIR and Milk proteins

ABSTRACT

This work focuses on studying the interaction between the active biomolecules found in turmeric and pepper with key milk proteins, which is a popularly adopted in the *Siddha*, one of the Indian Traditional Medicinal Systems, to treat cold and throat-related illnesses. Curcumin and Piperine are the active biomolecules in turmeric and pepper, respectively. Hence, we have analyzed their interaction with key milk proteins such as Bovine Serum Albumin (BSA), Lactaglobulin, and Lactalbumin. The interactions were computationally investigated to elucidate the underlying mechanism behind the efficacy of the aforementioned formulation using accurate first-principle calculations based on Density Functional Theory (DFT) and Molecular Docking simulations. The formation of the Curcumin-Piperine (CP) complex, as well as its binding with milk proteins, was evaluated using computational techniques. We have predicted the allosteric sites of the milk proteins and investigated the allosteric regulation effect in these proteins by Curcumin and Piperine. The results revealed the formation and increased bioactivity of the drug complex, thereby providing a molecular basis for the observed synergistic efficacy of this traditional formulation.

1. Introduction

Turmeric is one of the spices that people around the world have been using for ages. Curcumin is a yellowish dye, and it is the dominant phytochemical found in turmeric with the chemical alias Curcumin-(1,6heptadiene-3,5-dione-1,7-bis(4-hydroxy-3-methoxyphenyl)-(1E,6E) or feruloyl methane). Curcumin has a chemical composition of C₂₁H₂₀O₆, and it is a symmetric molecule with a molecular weight of 368.38 amu (Prasad and Aggarwal, 2011; Grykiewicz and Silfirski, 2012a2012; Priyadarsini, 2014a2014, 2013). It attracts pharmaceutical researchers due to its valuable health benefits, such as antibacterial, anti-inflammatory, antimicrobial, immunoregulatory, anti-oxidant, angiogenesis, anti-coagulation, anti-Alzheimer's, and chemotherapeutic applications. Curcumin is also shown to have anti-cancer properties (Grykiewicz and Silfirski, 2012b2012; Priyadarsini, 2014b2014; Ali et al., 2013; Esatbeyoglu et al., 2012; Mohan et al., 2000; Soleimani et al., 2018; Sharifi-Rad et al., 2020; Kuttan et al., 1985; Kuttan and Sudheeran, 1987). Along with Curcumin (C), two other chemical constituents are also found in turmeric, namely Demethoxy Curcumin (DMC), and Bis-demethoxy Curcumin (BDMC) which are collectively

called curcuminoids (Sharma et al., 2005. The molecular structure of curcuminoids is illustrated in Fig. 1. The heptadienone linkage between the Curcumin is less soluble in an aqueous environment, hence it has a solubility of less than 0.1 mg/mL at pH 7 and 18 $^{\circ}$ C, due to the presence of a hydrophobic aliphatic conjugated bridge. However, it may be soluble under an alkaline environment because of the presence of enolic and phenolic groups.

Although Curcumin has numerous benefits for human health, its low bioavailability and solubility (Solution Conformations of Curcumin in DMSO Cathryn et al., 2016; Siviero et al., 2015; Jeliński et al., 2019) makes it difficult to harness its potential pharmacological effect. When Curcumin is administered through the oral route, due to the presence of gastrointestinal enzymes such as proteases and peptidases, Curcumin is transformed into inactive metabolites that have a very low half-life by rapid degradation. Lin et al. conducted an *in-vivo* study of the metabolism of Curcumin on mice and found that Curcumin was bio-transformed into dihydro and tetrahydro Curcumin, subsequently, these two compounds were metabolized into the monoglucoronide conjugates (Pan et al., 1999 Apr). To cope up with these issues Curcumin must be co-administrated with certain bio-enhancers to promote its

E-mail address: vidyar@annauniv.edu (V. Ravindran).

a Centre for Materials Informatics (C-mAIn), Sir C.V. Raman Science Block, College of Engineering Guindy, Anna University, Chennai 600025, India

b Department of Physics, College of Engineering Guindy, Anna University, Chennai 600025, India

^{*} Corresponding author at: Centre for Materials Informatics (C-mAln), Sir C.V. Raman Science Block, College of Engineering Guindy, Anna University, Chennai 600025, India.

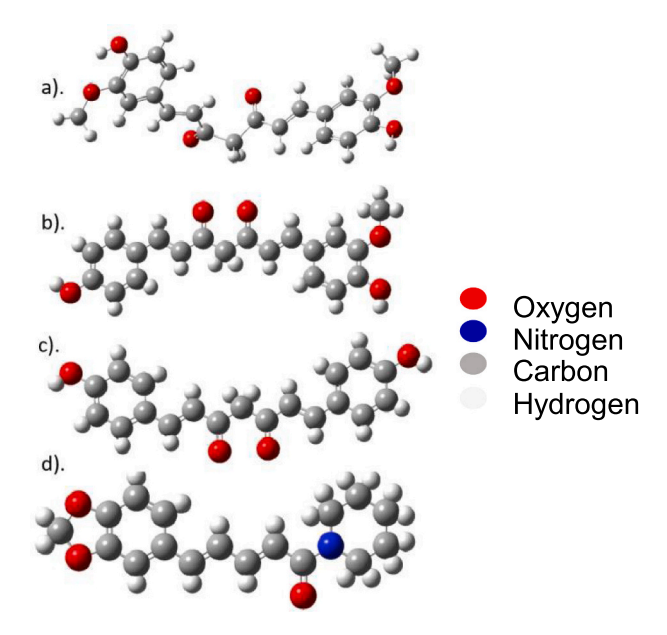


Fig. 1. Structures of a). Curcumin, b). Demethoxy Curcumin, c). Bis-Demethoxy Curcumin, and d). Piperine.

bioavailability through various ways.

Shoba et al. studied the effect of the combination of Curcumin and Piperine and evaluated the bioavailability of the complex in rats and human beings. Interestingly, bioavailability of the Curcumin was found to increase by 154 % and 2000 % in rats and humans, respectively (Shoba et al., 1998 May).

Piperine and milk proteins were previously reported to enhance the bioavailability of orally administered active pharmaceutical ingredients. Among such enhancers, Piperine is a heterocyclic phytochemical compound with a chemical composition of $C_{17}H_{19}NO_3$ found in all forms of pepper(Refer Fig. 1.d). It is the molecule responsible for the pungency and heat effect of the pepper. Piperine also has numerous beneficial effects on human health, such as anti-cancer, anti-diabetic, anti-obesity, cardio-protective, anti-microbial, anti-allergic, and anti-inflammatory properties (Lu et al., 2025.

It has the potential to inhibit most of the phase I (involves reduction, oxidation, hydrolysis reactions) and phase II (involves conjugation process) drug metabolizing enzymes such as Cytochrome P450, CYP3A4, and uridine diphosphate (UDP)-glucuronosyl transferases (UGT). Javed S et al. showed that an increase in bioavailability of silymarin (a drug used to treat liver disorders) with an increase in the concentration of Piperine by inhibiting the glucuronidation process (Javed et al., 2007. Indu Raghunath et al. stated that Piperine can be used as a bioenhancer to enhance the bioavailability of orally administered drugs (Raghunath et al., 2024. These works elucidate that the inhibition of drug-metabolizing enzymes can increase the gastrointestinal retention period and intestinal membrane fluidity. Thus, Piperine may be a good bio-enhancer (Khajuria et al., 2002.

Milk is the primary source of energy for the neonates of mammals, secreted by the mammary gland, able to meet the complete energy requirements of offspring. It is a major component in the human diet worldwide. Bovine milk is composed of proteins (containing essential & non-essential amino acids), fatty acids, vitamins, minerals, and a few minor nutritional factors. The protein content in milk may serve many physiological functions by acting as hormones, enzymes, enzyme inhibitors, and growth factors. Milk proteins are also reported to have many therapeutic benefits, ranging from anti-bacterial, anti-viral, anticarcinogenic to immunomodulatory properties, etc.; Davoodi et al. (2016); Haug et al. (2007); McSweeney and Fox (2009) The protein content in bovine milk is about 3.5 % by weight (36 g/L).

Milk proteins are primarily classified into two major groups: casein

and whey proteins. These are extensively characterized and have been studied more comprehensively than any other food proteins. In addition to these proteins, bovine milk also contains Proteose-Peptones(PPs), water-soluble protein-like molecules, and some nitrogenous compounds called Non-Protein Nitrogen (NPN). Bovine Serum Albumin (BSA), one of the whey proteins, also has a myriad of health benefits such as less toxicity, good bioavailability, scalability, low immunogenicity, better accumulation at tumor sites, and ease of administration (Bronze-Uhle et al., 2017; Yang et al., 2020; Solanki et al., 2021). We have investigated the interactions of Curcumin, Piperine and CP complex with whey proteins such as BSA, Lactalbumin (LA), and Lactaglobulin (LG).

Kumar et al. (2002) explored the use of natural biodegradable polymers such as chitosan and bovine serum albumin to create a depot drug delivery system. They employed an emulsion-solvent evaporation method combined with chemical cross-linking of polymers and develop the micro-spheres. Remarkably they achieved the encapsulation rate of about 79.49 % and 39.66 % for Curcumin within the albumin and chitosan carriers, respectively. This study strongly suggested that these Curcumin-loaded micro-spheres could serve as an effective prolonged-release delivery system, offering good therapeutic management to inflammatory conditions compared to oral and subcutaneous administration of Curcumin (Kumar et al., 2002 Apr). This study suggests that the milk proteins can acts as an effective drug delivery depot for orally administered drugs.

Additionally, in Siddha medicine, Curcumin is prescribed to be consumed with milk for relief from cold and throat-related issues. Additionally, it prescribes boiled milk with turmeric (*Curcuma longa*) and black pepper (*Piper nigrum*) as a formulation for cold and throat-related ailments. This traditional medication and its reported efficacy provided a strong rationale to conduct mechanistic studies into the synergistic interaction among Curcumin, Piperine, and milk proteins. In order to evaluate the interaction between Curcumin and Piperine, their combined interactions with milk proteins, we have used the state-of-the-art Density Functional Theory (DFT) calculations, docking simulations, and allosteric regulation prediction, which reveals the mechanism of action in the commonly consumed Siddha formulation.

2. Materials and methods

2.1. Identification and accession of structure of phytochemicals and proteins

All the chemicals mentioned in this work are identified through an extensive literature review. We searched to identify proteins and phytochemicals in the databases to obtain their respective three-dimensional molecular structure. Curcumin exists in different tautomerisms, such as Enol and Keto forms, and three different isomers, Curcumin, Demethoxy Curcumin and Bis-Demethoxy Curcumin. The structure of Curcumin (PubChem CID: 969516) and Piperine (PubChem CID: 638024) before optimization is shown in Figs. 1a and 1(d).

The crystal structure of milk proteins is obtained from the RCSB PDB database (URL: https://www.rcsb.org) (Berman et al., 2000. The crystal structures were chosen based on the presence of any mutation, resolution, and presence of specific ligands. The PDB IDs for α -Lactalbumin, β -Lactoglobulin, and BSA, respectively, are 1F6S (Chrysina et al., 2000, 3NPO (Loch et al., 2011, and 4F5S (Bujacz, 2012, respectively.

2.1.1. Density functional theory-based calculations

Density Functional Theory (DFT) is an advanced quantum mechanical technique to understand the electronic structure of molecules. DFT estimates the ground state energy of the molecule using self-consistent field (SCF) algorithm, which finds the ground state electron density. State-of-the-art Density Functional Theory (DFT) calculations are performed using the Gaussian-16 package (Gaussian 16 et al., 2016; GaussView, Version 6.1, 2016). The B3LYP (Becke-Lee-Yang-Parr)

Table 1Theoretical vs Experimental comparison of bond length and bond angle of Curcumin, other optimized geometry parameters are given in the supplementary information.

Bond Length			Bond Angle		
Bond	Theo.	Expt. Kolev et al., (2005)	Angle	Theo.	Expt. Kolev et al., (2005)
C ₁ -C ₂	1.410	1.417	C1-C2-C3	119.7	119.8
C2-C3	1.390	1.379	C_1 - C_2O_7	117.4	120.9
C2-O7	1.380	1.364	C_1O_8 - C_9	119.0	116.7
C3-C4	1.392	1.388	C_1 - C_6 - C_5	121.6	120.2
C4-C5	1.406	1.401	C_2 - C_1 - C_6	119.2	120.5
C5-C6	1.414	1.410	C_2 - C_1O_8	116.1	113.7
C6-C1	1.390	1.377	C_2 - C_3 - C_4	120.8	120.3
C1-O8	1.384	1.366	C_3 - C_4 - C_5	120.3	121.1
09-09	1.451	1.440	$C_4-C_5-C_6$	118.2	118.9
C5-	1.457	1.457	C ₆ -C ₅ -	118.9	119.7
C10			C ₁₀		
C10-	1.352	1.348	C ₅ -C ₁₀ -	127.9	128.3
C11			C ₁₁		
C11-	1.466	1.450	C ₁₀ -C ₁₁ -	121.6	121.5
C12			C_{12}		

method with the basis set 6-311 G (++) is implemented for all the quantum chemical calculations due to its highly precise outcome for the structure and thermodynamic attributes of polyphenolic compounds (Benchmarking Antioxidant-Related Properties for Gallic Acid through the Use of DFT, 2021; Boulmokh et al., 2023) and proximity between higher basis sets. The optimized geometry and electronic properties of Curcumin and Piperine were derived. The adsorption energy is calculated to study the possibility of adsorption between Curcumin and Piperine. Non-covalent interaction analysis and interaction region indicator analysis are carried out by applying the reduced density gradient method using the Multiwfn software (Lu and Chen, 2012. VMD tools (Humphrey et al., 1996 were used to visualize the predicted outputs of Multiwfn. Electrostatic potential(ESP) surfaces are obtained to provide a detailed perception of the binding sites. The vibration spectra of the Curcumin, Piperine, and the complex between Curcumin and Piperine (CP complex) were obtained with the same basis set to understand and confirm the complex formation.

2.1.2. Allosteric site prediction

Allostery is generally a functional and conformational modulation at one site resulting from a perturbation in a protein, which is reversible over time. Allostery or allosteric regulation plays a crucial role in maintaining cellular homeostasis through intra-protein communication processes, such as signal transduction, catalysis, and gene regulation. (Changeux, 2013; Liu and Nussinov, 2016). Thus, allosteric studies may open the door to understand the cause of the improved efficacy of Curcumin when co-administered with Piperine. Lu.et.al proposed a computational method to predict the allosteric site in a protein. They extracted the crystal structures of non-redundant proteins with greater resolution than 3 Å from the Allosteric Site Database (ASD) (He et al., 2024. They employed a discriminative feature selection method to identify key site descriptors that effectively represent an allosteric site. The collected data were used to train and optimize a support vector machine model and tested for allosteric site identification. The final model was made available on the web (http://mdl.shsmu.edu.cn/AST) for the detection of allosteric sites (Song et al., 2017. Using the AllositePro (2016), we predicted the allosteric sites in milk protein(s). For the predicted allosteric site, the docking studies were employed to shed light on the allosteric effect between milk protein(s) and small molecules.

2.1.3. Docking

We have used AutoDock Vina Software and the MGL tools package for docking simulation of ligands, including Curcumin, Piperine, and the CP complex with milk proteins. AutoDock Vina is one of the most

powerful & user-friendly open-access software for predicting the noncovalent binding of macromolecules like proteins and that of small molecules with proteins. It ultimately predicts the various possible bound conformations of a protein and small molecules. It works with the most effective Iterated Local Search Optimization algorithm, named the Broyden-Fletcher-Goldfarb-Shanno (BFGS), which is categorized as a quasi-Newton method. AutoDock Vina uses a machine learning-based scoring function, which includes some notable features of knowledgebased potentials and empirical scoring functions to approximate the chemical potential of the systems. AutoDock Tools from the MGL Tools Package was used for the preparation of receptors (proteins) accessed from the PDB database and ligands, by removing water molecules, adding polar hydrogens, repairing the missing atoms in the residues, and adding Kollman charges. All the grid boxes were generated with a grid spacing of 0.375 Å to define a search space for the software to find possible bound conformations of ligands with the proteins. All the simulations were run for the same grid spacing to ensure the comparability of the results (Trott and Olson, 2010. Protein-ligand interactions are visualized using UCSF Chimera software (Pettersen et al., 2004.

2.1.4. Limitations of computational methods used

The DFT calculations were performed under ideal conditions at 298 K and 1 atm. The absence of an explicit solvation environment may influence the interaction strength of the molecules. In physiological conditions, the interaction of Curcumin, Piperine, and the CP complex could be affected by both temperature and solvation effects in the gut. For calculating the spectroscopic parameters such as FTIR frequencies, DFT has not accounted for the anharmonic vibrations, which will lead to a slight variation in peaks when compared to the experimental values. Moreover, as docking algorithms are non-deterministic in nature, the results may vary slightly each time the docking is performed, even with the same input parameters.

3. Result and discussion

3.1. Molecular structure optimization

The geometry optimizations were carried out on both Curcumin, Piperine, and the CP complex. The molecules were initially placed within an intermolecular distance of 1.8 Å, ensuring a conducive environment for non-covalent interactions. Co-optimization was done to explore all possible bound coformations, allowing relaxation of molecular geometries to achieve the convergence to find the minimum energy structure. A total of 37, 19, and 116 conformations were generated, respectively, out of which the conformers with the lowest global minimum energy were chosen. The global minimum energy for Curcumin, Piperine, and CP complex are −1263.54 Hartree and −939.61 Hartree, and -2203.17 Hartree, respectively. The geometry parameters, such as bond lengths and bond angles of the Curcumin, were compared with the parameters obtained from the single crystal XRD, and proximity between the experimental and theoretically derived parameters was found to be in good agreement as given in Table1. Geometry parameters of Curcumin, Piperine, and CP complex are provided in supplementary section. The optimized molecular structures are given in Fig. 2.

A modest expansion of the geometry parameters, including bond length and bond angles, was indicated by the average change in the bond length of Curcumin and Piperine following optimization, which was of the order of 0.01 Å in both cases. However, in the CP complex, the bond length and angles were reduced, with the average change in bond length of 0.02 Å compared to those in the individual molecule.

Moreover, the attractive interaction with the hetero ring of Piperine at both moieties caused the angle between the Curcumin's arms to decrease by 0.40° and the bond length of OH in the aromatic ring (Ring 1) of Curcumin to extend by 0.013 Å.

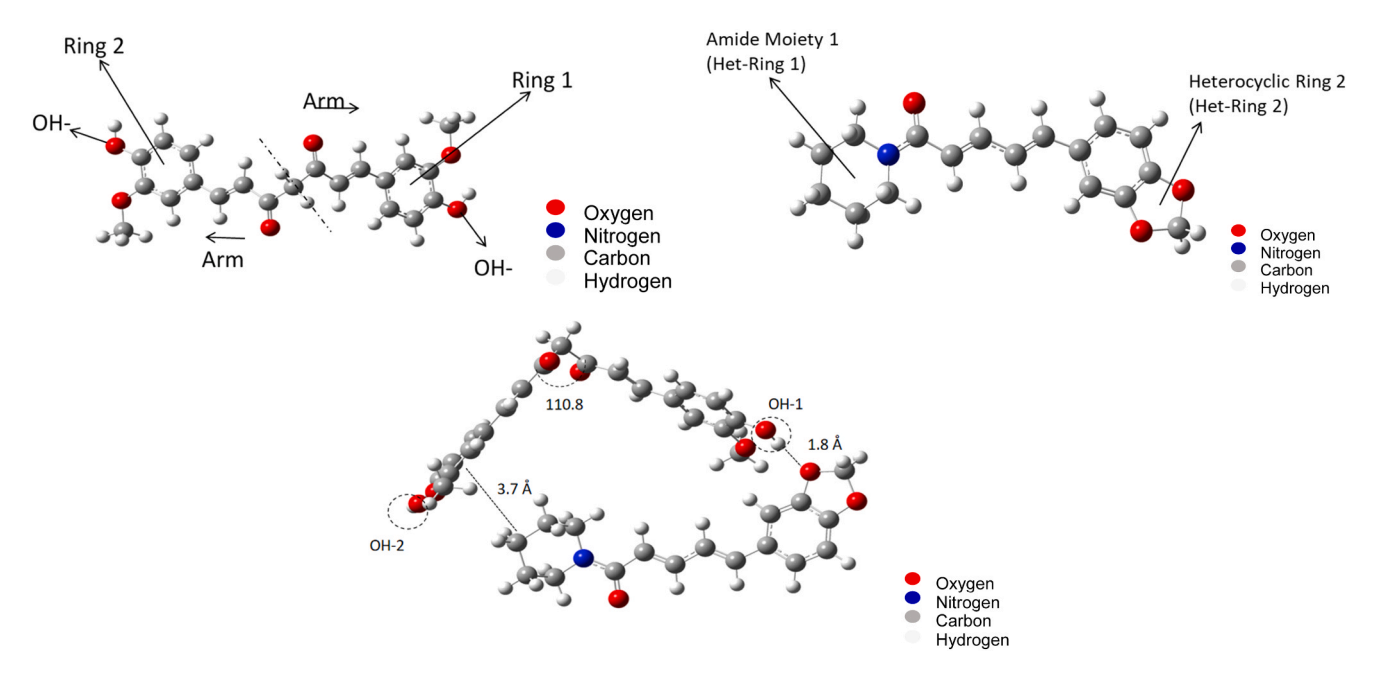


Fig. 2. (a). Optimized structure of Curcumin using B3LYP basis set, Fig. 2(b). Optimized structure of Piperine using B3LYP basis set, Fig. 2(c). Optimized structure of Curcumin-Piperine (CP) complex using B3LYP basis set. The formation of hydrogen bonding between the Curcumin and Piperine is highlighted by the dotted circles.

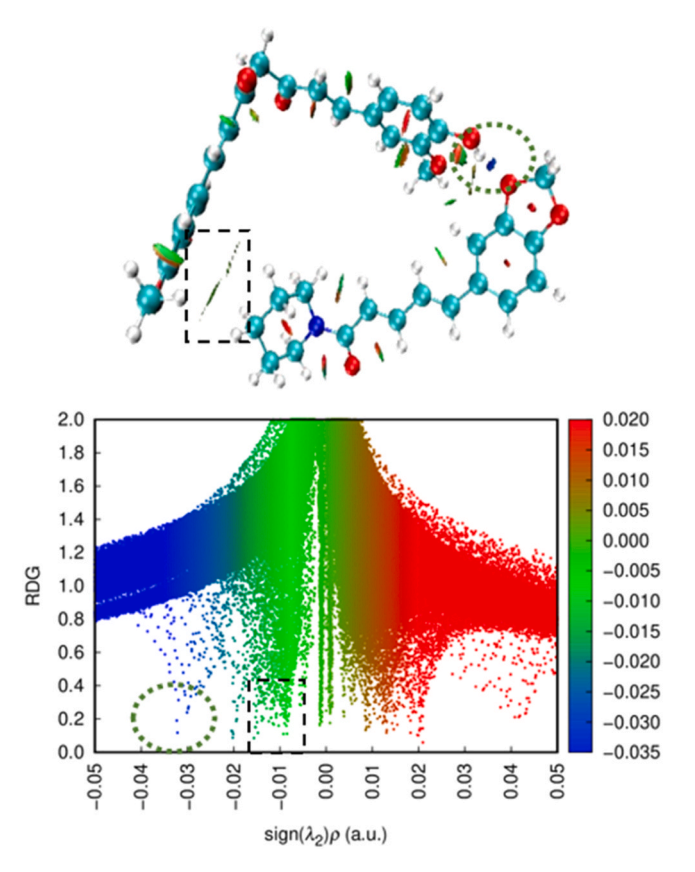


Fig. 3. NCI analysis-Reduced Density Gradient Scatter plot: Blue peaks (Indicated by circle) corresponds the hydrogen bond and Green peaks (Indicated by square) correspond to Van Der Waals Interaction.

3.2. Adsorption energy

Adsorption energy calculations were done on the CP complex to assess the stability of the adsorbed species using the following Eq. (1).

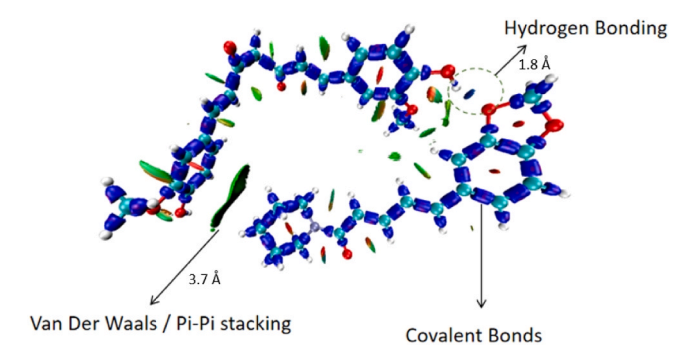


Fig. 4. Interaction Region Indicator (IRI) module reveals the region where the interaction takes place between Curcumin and Piperine in the CP complex.

$$E_{Adsorption} = E_{Complex} - (E_{Piperine} + E_{Curcumin})$$
 (1)

The negative adsorption energy indicates that the adsorption is energetically favorable, whereas a positive value indicates adsorption is not energetically favorable. The larger the negative adsorption energy indicates the stronger the adsorption (Ganji, 2015.

In Eq.(1), $E_{Complex}$ is the total energy of the CP complex, and $E_{Piperine}$ and $E_{Curcumin}$ are the total energies of individual Piperine and Curcumin molecules. The CP complex exhibits an adsorption energy of -12.6 kcal/mol. This adsorption energy value suggests the existence of physisorption between the Curcumin and Piperine. i.e., non-covalent interactions such as hydrogen bonding, Van der Waals forces, π - π interactions between the Curcumin and Piperine molecules, could be the reason for the CP complex formation.

3.3. Non-covalent interactions (NCI) analysis

The Non-Covalent Interaction (NCI) analysis can provide crucial insights into the binding mechanism between Curcumin and Piperine. This analytical technique elucidates the nature and strength of the non-covalent interactions, which play a critical role in the drug delivery efficiency and stability. The NCI are classified by the sign of the second density Hessian eigenvalue (λ_2), λ_2 0 < 0 (blue coloured) for attractive

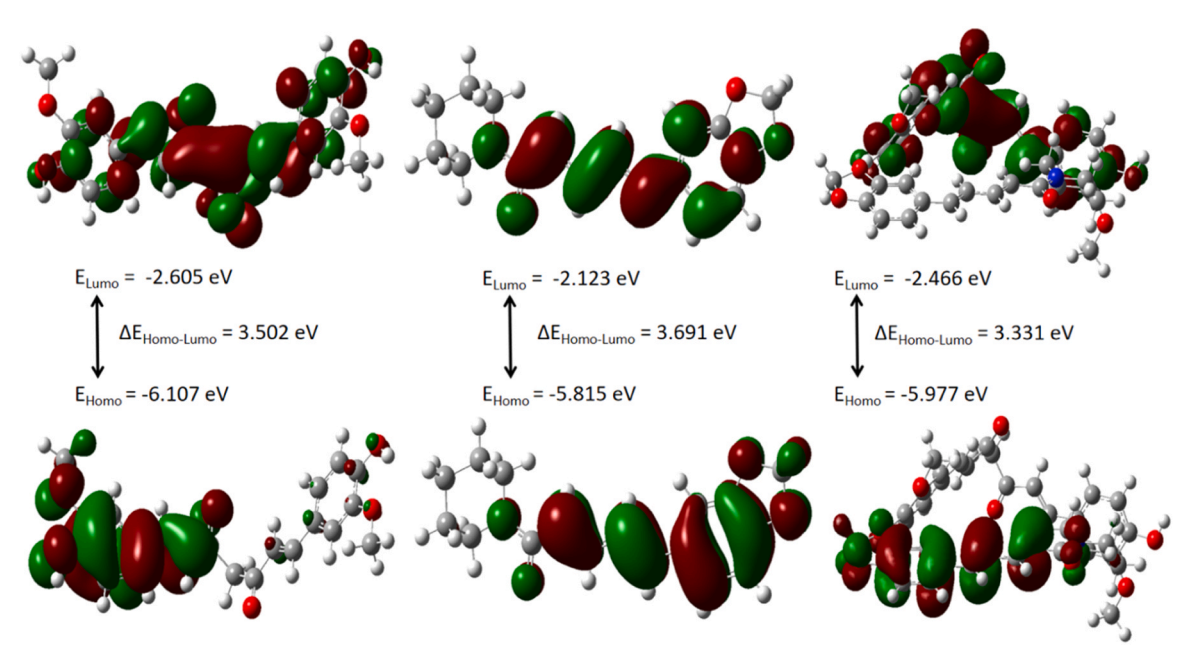


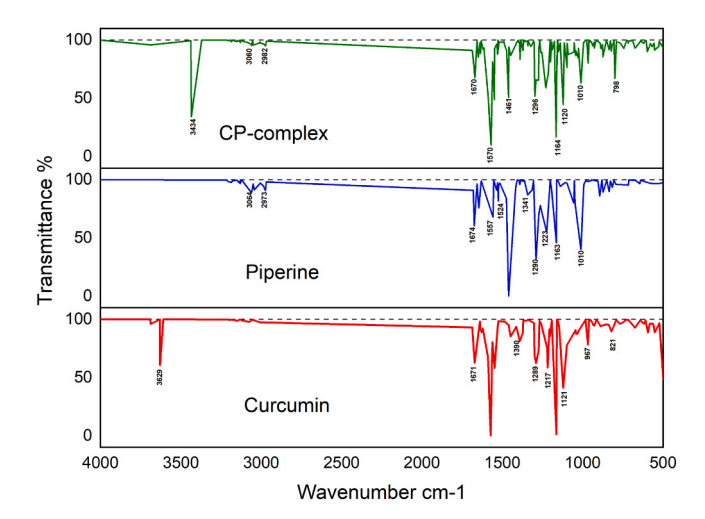
Fig. 5. Frontier Molecular Orbital analysis of Curcumin, Piperine, and CP complex. The positive and negative orbital lobes are represented in green and red colour respectively.

Table2Chemical reactivity parameters of Curcumin, Piperine, and CP complex.

Properties	Curcumin	Piperine	CP complex		
E _{Homo} (eV)	-6.107	-5.815	-5.977		
E _{Lumo} (eV)	-2.605	-2.123	-2.646		
$\Delta E_{(Homo-Lumo)}$ (eV)	3.502	3.691	3.331		
Hardness (η, eV)	1.751	1.846	1.665		
Softness (σ , eV ⁻¹)	0.571	0.542	0.600		
Electronegativity (χ, eV)	4.356	3.969	4.312		
Chemical Potential (µ, eV):	-4.356	-3.969	-4.312		
Electrophilicity Index (ω, eV)	5.420	4.268	5.581		
Electrophilicity Power (ϵ , eV ⁻¹)	0.185	0.234	0.179		

interactions, $\lambda_2 > 0$ (red coloured) for repulsive interactions (Otero-de-la-Roza et al). In the context of Curcumin and Piperine, NCI analysis can reveal how these two chemicals can interact with each other.

The NCI method relies on two scalar fields to map the bonding



 ${\bf Fig.~6.}$ Theoretically generated FTIR spectra of Curcumin, Piperine, and CP complex.

properties: the electron density ρ and reduced density gradient (RDG, denoted by "s") defined in Eq. 3.

$$(RDG)s = \frac{1}{2(3\pi^2)^{\frac{1}{3}}} \frac{|\Delta \rho(r)|}{\rho(r)^{\frac{4}{3}}}$$
 (3)

RDG is a measure of how the electron density varies in space. The regions with smaller RDG values correspond to non-covalent interactions. The combination of s and ρ describes the nature of the bonding. High-s low- ρ corresponds to non-interacting regions, low-s high- ρ to covalent bonds, and low-s low- ρ to non-covalent interactions. Using s, ρ , and λ_2 , this method offers a detailed characterization of the spatial regions where non-covalent interactions occur and their corresponding intensity.

For visualizing the interaction regions in the CP complex structure, we employed the Interaction Region Indicator (IRI) module in Multiwfn (Lu and Chen, 2012, which is capable of clearly identifying both chemical bonds and weak interaction regions. The CP complex demonstrates the existence of hydrogen bonding between the OH-1 group of the Phenolic ring of Curcumin and hydrogen in the heterocyclic ring of Piperine. As seen in Fig. 3.

The strength of a hydrogen bond is direction dependent, i.e., the angle formed by the hydrogen atom and the two electronegative atoms affects its strength because of the dipole's ideal alignment. The hydrogen bond is stronger when this angle gets closer to 180° . In the CP complex, the angle between OH···O is 171° , resulting in a strong hydrogen bond. Apart from the hydrogen bonding between the C and P, the IRI also revealed that Van der Waals interaction exists between the ring 2 of Curcumin and the amide moiety (Het-Ring 1) of Piperine in the CP complex, as shown in Fig. 4.

3.4. Mulliken charge analysis

Mulliken charge analysis is a computational approach used to analyze the distribution of electrons in molecules and assign partial atomic charges based on molecular orbital theory (Mulliken, 1939; Arivazhagan et al., 2015). It is crucial for elucidating molecular properties of the system, including electronic structure, reactivity, dipole moment, polarization, and vibrational spectrum, using quantum chemical calculations. Millikan charges were tabulated in the supplementary

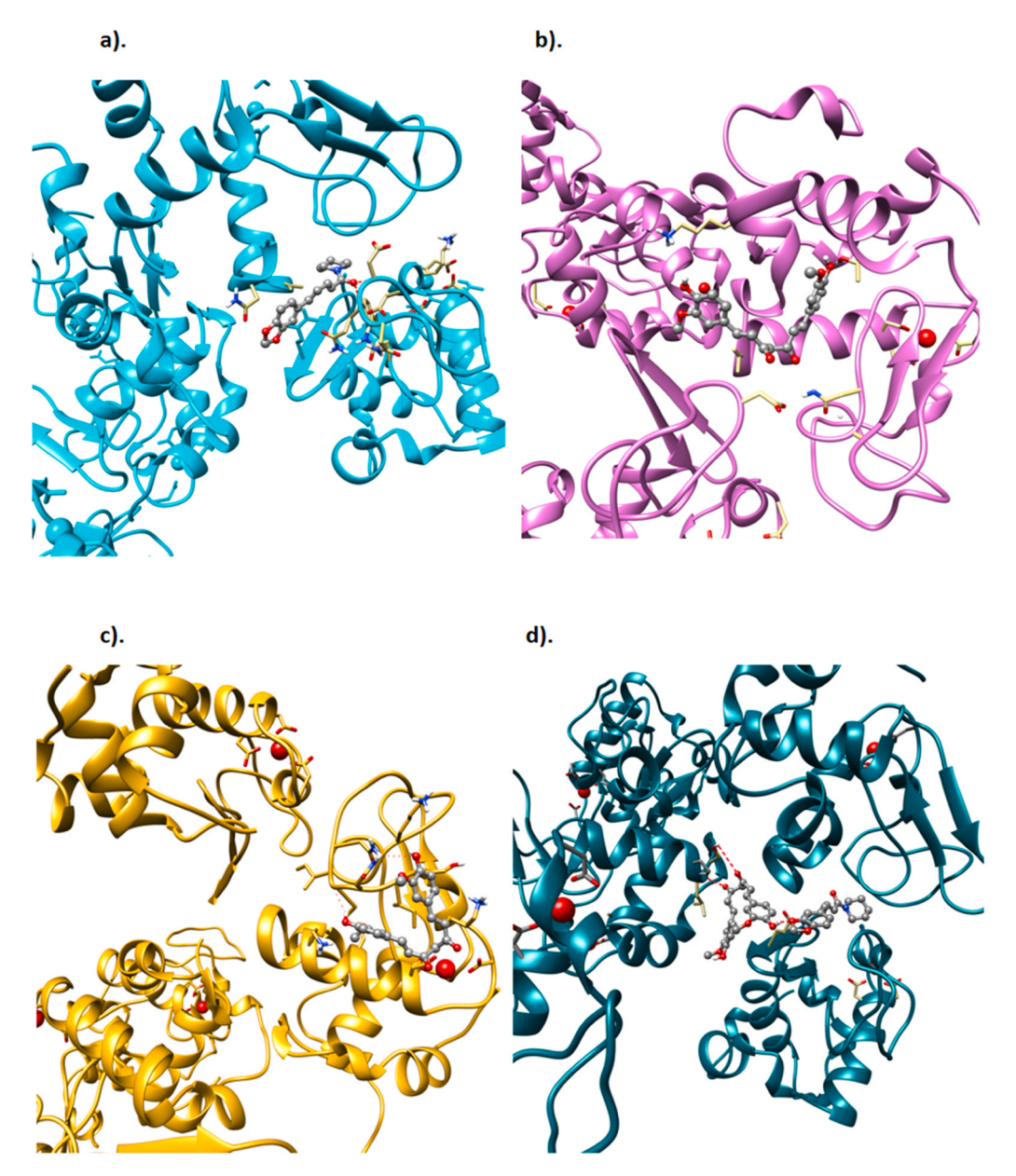
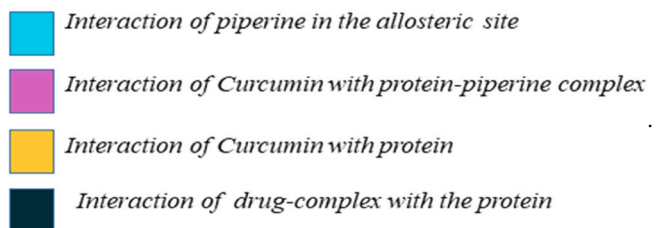


Fig. 7. a)Interaction of Piperine in allosteric site of lactalubumin, b). interaction of Curcumin in lactalubumin-Piperine complex, c). interaction of Curcumin in unliganded lactalubumin, d). interaction of CP complex in lactalubumin.Colouring scheme: in all three interaction profile, we have used the following colouring scheme:



information. In the Curcumin and CP complex, the electron density around the carbon atoms (C_7 , C_{10} , C_{12} , C_{14} , C_{18} , C_{22}) alters as a result of the hydrogen bond that is formed between the Curcumin and Piperine molecules. However, there is a considerable change in the charge distribution on the hydroxyl group of Curcumin, where an H-bond is formed. In a hydroxyl group, the charges of hydrogen and oxygen range from 0.38 to 0.57 and -0.55 to -0.65, respectively. The changes in atomic charges will reflect in the vibrational spectrum and electronic

structure of the molecule since it is directly related to the chemical bond present in the molecule.

3.5. Frontier molecular orbital analysis

Frontier molecular orbitals (FMOs), which include the Lowest Unoccupied Molecular Orbital (LUMO) and the Highest Occupied Molecular Orbital (HOMO), are essential in quantum chemistry and the FMOs

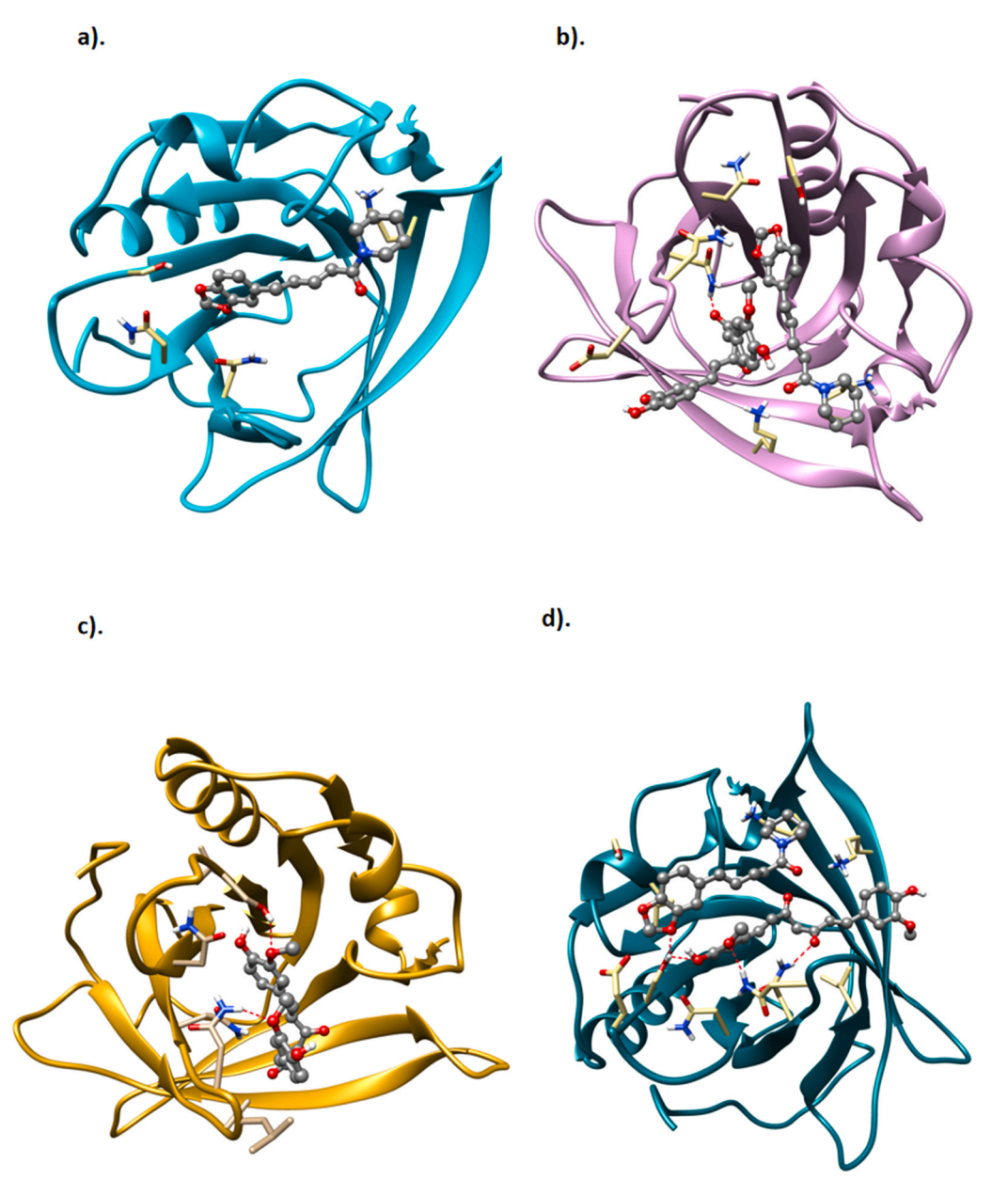


Fig. 8. a)Interaction of Piperine in allosteric site of lactoglobulin, b). interaction of Curcumin in lactoglobulin-Piperine complex, c). interaction of Curcumin in unliganded lactoglobulin, d). interaction of CP complex in lactoglobulin.

determine a material's electronic structure and optical properties (Gupta et al., 2011. The HOMO, which contains the electrons, acts as an electron donor and indicates a molecule's vulnerability to electrophile attack, while the LUMO acts as an electron acceptor and shows how vulnerable a molecule is to nucleophile attack. The $E_{HOMO}\text{-}E_{LUMO}$ gap ($\Delta E_{HOMO-LUMO}$), which is the difference between the E_{LUMO} and E_{HOMO} energies, aids in determining the molecule's chemical reactivity and kinetic stability. The higher the $\Delta E_{HOMO-LUMO}$ gap, stability is more stability and reactivity is less compared to a system with a low gap. The $\Delta E_{HOMO-LUMO}$ of Curcumin, Piperine, and the CP complex are given in Fig. 5. E_{HOMO} , E_{LUMO} , $\Delta E_{HOMO-LUMO}$, and other chemical reactivity parameters (Ouaket et al., 2022 of Curcumin, Piperine, and the CP complex are tabulated in Table 2.

In the CP complex, the Curcumin acts as a donor and Piperine as an acceptor. Curcumin engages in hydrogen bonding through a shared hydrogen atom, resulting in a partial positive charge on Curcumin due to the polarization of bonds. This charge redistribution corresponds with the localization of the LUMO on Curcumin. In contrast, Piperine exhibits

electron-rich character, favoring HOMO localization on Piperine.

In the complex, the overall E_{HOMO} is raised to -5.977 eV, indicating that Curcumin contributes significantly to the shared molecular orbital of the complex. The formation of a hydrogen bond stabilizes the E_{LUMO} , which is a reason for the E_{LUMO} of the CP complex lies intermediate E_{LUMO} of the individual molecules. The change in the $\Delta E_{HOMO-LUMO}$ of the complex reflects the effective charge transfer between the donor and acceptor and facilitating electronic transition and altering the complex's properties. This low $\Delta E_{HOMO-LUMO}$ also implies that the complex is biologically more active than individual molecules, facilitating its participation in charge transfer, hydrogen bonding, or covalent bonding with the biomolecules.

The chemical reactivity parameters can be derived from the $\Delta E_{HOMO\ LUMO}$. For example, it gives insight into the nature of a molecule and the formation of a molecular complex. The electronegativity of the CP complex is found to be 4.312 eV, which is less than the electronegativity of Curcumin and Piperine, suggesting there is a shifting of charges between Curcumin and Piperine that might cause the change in the overall

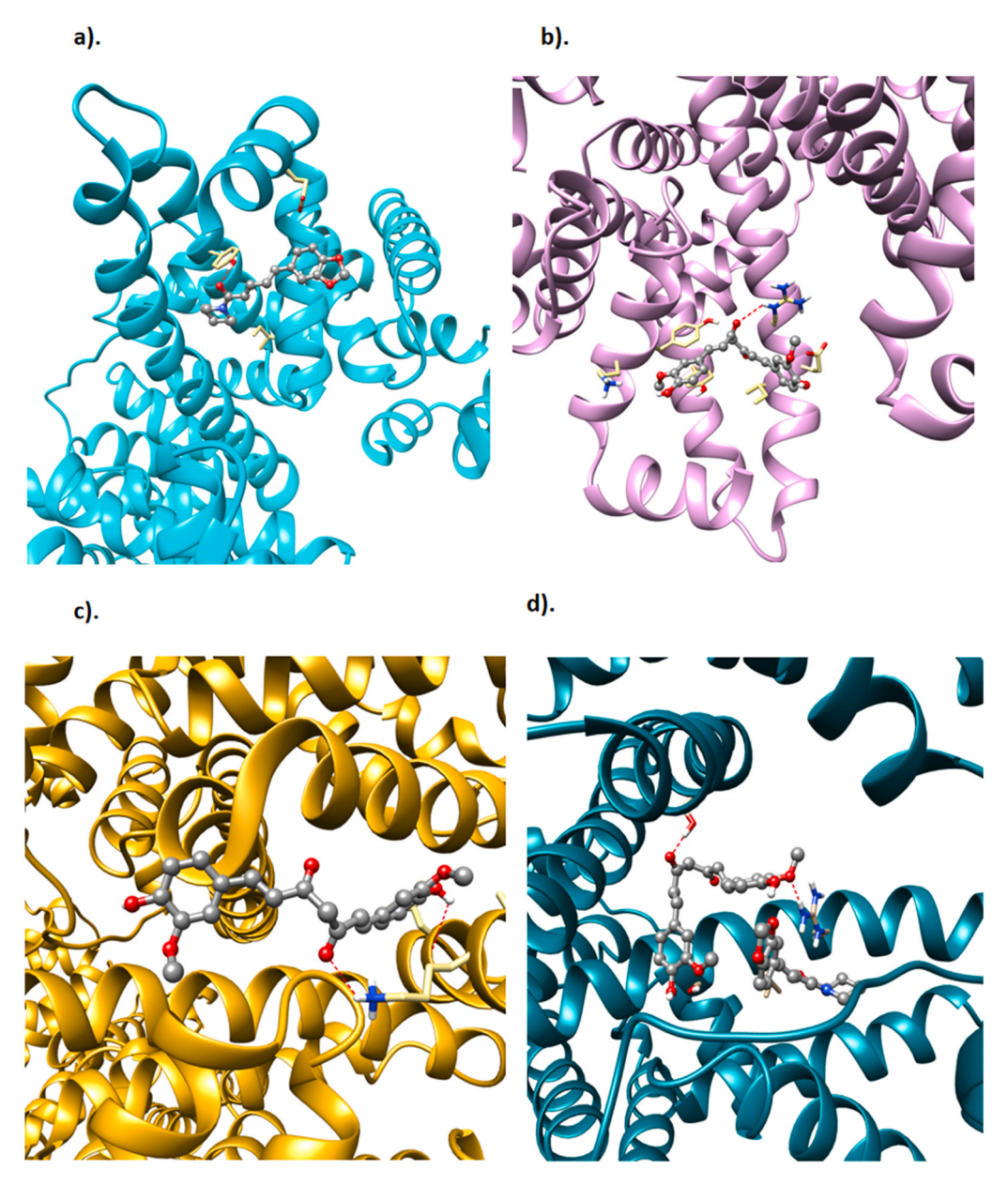


Fig. 9. a)Interaction of Piperine in allosteric site of BSA, b). interaction of Curcumin in BSA-Piperine complex, c). interaction of Curcumin in unliganded BSA, d). interaction of CP complex in BSA.

electronegativity of the molecular complex.

3.6. FTIR spectra

In order to further confirm the formation of a hydrogen bond between the Curcumin and Piperine in the CP complex, we carried out the vibrational energy calculations using Gaussian 16 with the 6311 G+ + level of theory and methanol solvation. The theoretically generated spectra are presented in Fig. 6. Experimental data for Curcumin show good agreement with those given in Table 3. A slight deviation in the peaks between the experimental and theoretical data can be attributed to the neglect of anharmonic effects in the simulated molecular vibrations. The intermolecular interactions, such as hydrogen bonding, London dispersion forces, and van der Waals forces, can cause shifts and splitting of vibrational levels.

The computed vibrational frequencies of Curcumin are observed at $3215~{\rm cm}^{-1},~3012~{\rm cm}^{-1},~and~3003~{\rm cm}^{-1},~for~Piperine,~observed~at~3133~{\rm cm}^{-1}$. Since the vibrational frequencies involved in C-H stretching

generally range from $2860 \text{ to } 3200 \text{ cm}^{-1}$, these observed vibrations could result from C-H stretching.

The C=O stretching ranges from 1550 to $1850~\rm cm^{-1}$. The computed frequencies of C=O stretching vibrations for Curcumin are observed at $1628~\rm cm^{-1}$ for Piperine at $1674~\rm cm^{-1}$, and the same is observed for the CP complex.

The O-H stretching frequencies are usually observed between 3200 and 4000 $\rm cm^{-1}$. The computed frequencies of O-H stretching vibrations for Curcumin are 3629 $\rm cm^{-1}$ and 3687 $\rm cm^{-1}$, and the CP complex is 3434 $\rm cm^{-1}$ and 3687 $\rm cm^{-1}$.

The free hydroxyl group of Curcumin vibrates at the frequency of 3689 cm⁻¹ and 3629 cm⁻¹, but in the complex, the OH stretching frequency is shifted to 3434 cm⁻¹, which suggests that the hydroxyl group is involved in an interaction with Piperine. This peak shift is caused due to the formation of a hydrogen bond between the compounds, which weakens the O-H bond, leading to elongation of the O-H bond, thus lowering the O-H vibrational frequency. The drop of 255 cm⁻¹ may suggest a moderate to strong hydrogen bond.

Table 3The calculated vibrational frequencies of the FTIR spectra of Curcumin and the experimental counterparts values.

Wavenumber(cm ⁻¹)		Band Assignment		
Theoretical	Experimental (Kolev et al., 2005			
3629	3512	ν(O-H), rings		
3687	3590	ν(C-H), rings		
1450	1486	(OC-H), rings + δ (OC-H), rings		
		$+ \nu$ (C = C), rings $+ \delta$ (C-H), rings/chain $+ \delta$ (O-H), rings/enol group		
1390	1428	ν (C = O), enol group + δ (O-H), enol group/ rings + α (O-H) rings + α (O-H)		
1218	1232	chain $+\delta$ (OC-H) rings $+\nu$ (C = C), chain ω (OC-H), rings $+\delta$ (OC-H), rings $+\delta$ (C-H), rings $+\delta$ (C-H), rings/chain		
1165	1183	δ (O-H), rings + δ (C-H), rings + δ (OC-H), rings		
1119	1151	δ(C-H), rings/chain		
1030	1026	ν (C-C), chain + γ (C-H), chain + δ (C-H), rings + α (C-H), rings		
818	834	γ (C-H), rings/chain + γ (O-H), enol group + ν (C = C), rings + ν (C-C), rings		

The aromatic C=C stretching vibration, observed at $1494~cm^{-1}$ in individual Curcumin, shifts to $1415~cm^{-1}$ in the complex. This shift indicates the relaxation of the C=C bond in Curcumin, which occurs due to the redistribution of the electron density in the aromatic ring of Curcumin, further supporting the formation of π - π stacking interactions between the OH-2 and phenolic rings of Curcumin and Piperine.

3.7. Interaction of Curcumin, Piperine, and complex with milk proteins

3.7.1. Interaction of Curcumin, Piperine, and bound complex with lactalbumin

The docking scores for the protein-ligand complexes are given in Table 4. In the case of α -Lactalbumin, which contains 6 subunits, namely A, B, C, D, E, and F. Three allosteric sites were predicted, and two of them are located in Chain-F and one is located in Chain E. The binding affinity of Piperine with the allosteric site is -7.2 kcal/mol. The binding is more favorable in the interfacial region of the D and F chains of the protein. Piperine has formed three hydrogen bonds with the residues present inside the binding pocket, which is present in the subunit interface region of the protein. Then the binding of Curcumin with this protein-Piperine complex is analyzed, and the binding energy is predicted to be -6.0 kcal/mol by forming a single hydrogen bond with the residue in the binding pocket.

Now, we have simulated another docking to understand the effect of Piperine in the allosteric site on the binding of Curcumin with the protein. A blind docking of the protein in its unliganded form is performed, and the binding affinity of Curcumin with the protein is found to be $-5.5~\rm kcal/mol$ with the formation of three hydrogen bonds on the surface region of the proteins in the same Chain-F. The binding energy reveals that the presence of Piperine in the allosteric site enhances the binding of Curcumin with the protein. We have also confirmed that the Piperine and Curcumin interact with the same subunits that form the allosteric mechanism during ligand binding.

To understand the combinatorial effect of ligands, we have optimized the molecular complex formed by Curcumin and Piperine using the DFT framework as mentioned earlier. The binding affinity of this molecular C-P complex with the protein is $-10.5\,\mathrm{kcal/mol}$ with the formation of three hydrogen bonds. The complex is bound in the region of the interface between three subunits, namely D, E, and F, and the binding is further stabilized by 4 hydrophobic interactions. Additionally, there is a π - π stacking (T-Shaped) interaction between the aromatic rings of Curcumin and the Phenylalanine residue present in the Chain-E. This binding affinity is relatively higher than any other combination of

ligands with the protein, suggesting that the binding of the ligand complex is more favorable. It is suggested that the formation of a molecular complex and the binding of this complex with the protein may lead to the enhanced bioavailability of Curcumin, since the possibility of getting degraded by the gut enzymes will be low in its bound form compared to the free forms of ligands.

3.7.2. Interaction of Curcumin, Piperine, and bound complex with lactoglobulin

In the case of β -Lactoglobulin, the same order of docking simulations has been performed. The protein has only one chain, A, and the allosteric site was predicted with a volume of 165 Å. The same procedure has been followed as mentioned earlier. The binding affinity of Piperine with the protein is -6.2 kcal/mol. In this case, no hydrogen bond is formed between the Piperine and the residues present in the protein. Hydrophobic interactions are present, as mentioned in Table 4.

The binding affinity of Curcumin with the complex formed by the protein and Piperine is $-6.4\,\mathrm{kcal/mol}$. Here, Curcumin forms two hydrogen bonds with the protein. The binding of Curcumin in the unliganded form of the protein was also carried out, and the binding affinity was found to be $-6.3\,\mathrm{kcal/mol}$ with the formation of 4 hydrogen bonds. There is a decrease in binding affinity, which confirms that the binding of Curcumin is more favorable when the Piperine is bound within the allosteric site of the protein, which may stabilize the interaction of Curcumin with the protein.

When the binding of the Curcumin-Piperine complex is analyzed, there is an increase in binding energy, at $-8.6~\rm kcal/mol$ with 3 hydrogen bonds. Here, we also confirm that the binding of the molecular complex may reduce the degradation of the drug by the gut enzymes. In essence, the gastroretention of the drug complex in its bound form, along with the milk protein, may increase compared to its free form, resulting in increased efficiency of its pharmacological effects.

3.7.3. Interaction of Curcumin, Piperine, and bound complex with Bovine Serum Albumin

In the case of BSA, which is a dimeric protein with 2 chains A and B, two allosteric sites with a pocket volume of 3576 Å and 1139 Å were predicted in chain A. The binding of Piperine was detected in chain A in the region of the interface of both chains bound within a deep pocket with a binding affinity of $-7.5~\rm kcal/mol$. The binding of Piperine in the deep pocket is stabilized by 2 hydrogen bonds and 9 hydrophobic interactions with the residues present in chain-A. This high number of hydrophobic interactions may be due to the fact that Piperine is bound inside a deep pocket rather than on the surface.

Then we have carried out a docking simulation to understand the binding of Curcumin with the protein-Piperine complex to understand the effect of the presence of Piperine in the allosteric site. The binding affinity is found to be $-8.0\,\rm kcal/mol$ with 1 hydrogen bond per ligand and 15 hydrophobic contacts contributed by both ligands from chains A and B. The quite large number of hydrophobic interactions and the attachment of ligand in the deep and interfacial regions of protein subunits may lead to an increase in the binding energy of Curcumin in BSA compared to other proteins, as discussed earlier.

The docking simulation to understand the binding of Curcumin with the protein showed a binding affinity of -6.3 kcal/mol. The decrease in binding energy shows the presence of Piperine is playing a prominent role in increasing the binding efficiency of Curcumin in all the abovementioned proteins. Curcumin forms 2 hydrogen bonds with the residues in chain B. The binding of the Curcumin-Piperine complex has a binding energy of -11.2 kcal/mol, as expected from the previous cases. The binding is stabilized by forming 6 hydrogen bonds and 8 hydrophobic interactions. Additionally, there is a presence of π -cation interaction between the aromatic ring of Curcumin with the positively charged Arginine residue, with a distance of 3.95 Å. Here, the Curcumin-Piperine complex is bound to the deep binding pocket present in the Chain-B, resulting in higher binding energy.

Table 4 Binding profile and key interacting residues for α -Lactalbumin, β -Lactoglobuin, and Bovine Serum Albumin (BSA).

Protein and Details of Allosteric Sites	Interacting units	Binding energy kcal/ mol	Hydrogen bonds	Bond distance	Hydrophobic interactions
α-Lactalbumin 3 Allosteric sites of volumes	Binding of Piperine in the predicted allosteric sites. Docking of Curcumin with the protein and Piperine complex	-7.2	TYR-50D, ASP-64D, GLN-65D	3.28, 2.57, 2.22	GLN-65D, ILE-59F, TYR-103F, VAL-99F, TRP-60F, ASN-102F and LEU-105F.
2199 Å, 1663 Å, and 322 Å. (Chains A, B, C, D, E, and F) (Refer to Fig. 7)		-6.4	ALA-106F	3.3	THR-33F and LEU-105F.
(1000 00 00)	Docking of protein and Curcumin without Piperine in the allosteric site.	-5.5	ASN-74F, ASN-74F, LYS- 94F	2.14, 3.44, 2.82 Refer to Fig. 3	ILE-75F(3 Interactions), LYS-79F, ASP-87F
	Docking of Curcumin and Piperine complex with protein.	-10.5	Interaction of Curcumin LYS-13E, LEU-23E, ASN-45D	2.45, 2.06, 2.48	PHE–9E, LEU–119E(2 Interactions), PHE–9E-π-Stacking (perpendicular)
			Interaction of Piperine	-	Chain-D ASP-64
β-Lacto globulin 1 Allosteric site of volume	Binding of Piperine in the predicted allosteric sites.	-6.2	-	-	LEU-31A, LEU-39A.
165 Å. (Chain-A) (Refer to Fig. 8)	Docking of Curcumin with the protein and Piperine complex	-6.4	Interaction of Piperine: -	-	LEU-31A, LEU-39A.
. 0	•		Interaction of Curcumin: LYS-69A, ASN-90A	2.71, 1.98	ILE-71A, ALA-86A.
	Docking of protein and Curcumin without Piperine in the allosteric site.	-6.3	ASN-88A, ASN-109A, SER-116A(2 Hydrogen bonds)	2.27, 2.64, 2.41 and 2.12.	LEU-39A, ALA-86A, LEU-87A, ASN-88A.
	Docking of Curcumin and Piperine complex with	-8.6	Interaction of Piperine SER-116A	2.16	LEU-31A, PRO-38A
	protein.		Interaction of Curcumin ASN-88A, ASN-90A.	2.14, 2.28.	LEU-39A, ILE-84A.
Bovine Serum Albumin (BSA) 2 Allosteric sites of volume 3576 Å and 1139 Å.	Binding of Piperine in the predicted allosteric sites.	-7.5	Interaction of Piperine LYS-136A, TYR-160A	2.97, 2.10	LEU-115A, PRO-117A, LEU-122A, LYS-136A, TYR-137A, ILE-141A, TYR-160A, ILE-181A, and ARG-185A.
(Chain-A and B) (Refer to Fig. 9)	Docking of Curcumin with the protein and Piperine complex	-8.0	Interaction of Piperine LYS-116A	2.94	LEU-115A(2 interactions), PRO-117A, THR-121A, PHE-133A(2 interactions), LYS-136A, and TYR-160A.
	•		Interaction of Curcumin ARG-185B	3.27	LEU-115B(2 interactions), PRO-117B, TYR-137B, ILE-181B, GLU-182B and ARG-185B
	Docking of protein and Curcumin without Piperine in the allosteric site.	-6.3	LEU-346B, LYS-350B	2.41, 2.44	PHE- 205B, LEU- 346B, LYS- 350B, VAL- 481B
	Docking of Curcumin and Piperine complex with	-11.2	Interaction of Piperine Arg-185B	3.52	LEU-115B, ILE-141B, ARG-144B, TYR-160B, and ARG-185B.
	protein.		Interaction of Curcumin HIS-154B, Arg-185B, Arg-185B, SER-192B, SER-428B	2.44,2.95,1.91, 2.86, 1.92	LEU $-189B$, ILE $-455B$, and ARG $-458B$. π -Cation interaction between Curcumin and ARG $-458B$

From all the docking simulations, we found a similarity that the molecular complex has more reactivity than the individual molecules (Refer to Table 4 for binding energies of the ligands). From the FMO analysis, it is clear that the higher reactivity of the molecular complex is one of the influencing factors in the binding affinity of the complex with milk proteins.

4. Conclusions

We performed DFT calculations and molecular docking simulations to investigate the interaction of Curcumin and Piperine with the milk proteins. DFT analysis confirmed the formation of a stable Curcumin-Piperine (CP) complex, stabilized by noncovalent interactions such as hydrogen bonding and $\pi\text{--}\pi$ stacking interactions, with an adsorption energy of $-12.6\,\text{kcal/mol}$. The optimized structural parameters and stimulated FT-IR spectra exhibit proximity with reported experimental data, validating the computational approach. Reduced Density Gradient (RDG) analysis further supported the existence of non-covalent interactions within the CP complex.

Docking Studies revealed that the CP complex exhibited the strongest affinity toward BSA. This suggests the role of BSA as a potential carrier by encapsulating the CP complex within deep binding pockets. Binding analyses also indicated the enhanced cooperative binding of the CP complex in the binding pockets of the proteins. FMO analysis elucidates the higher reactivity of the CP complex due to the reduced HOMO-LUMO gap, which in turn results in the stronger binding affinity of the complex over the individual counterparts.

From a pharmacokinetic perspective, the bioavailability of Curcumin is improved through multiple mechanisms: Piperine acts as an inhibitor of metabolic enzymes in the gut, prolonging the retention time of Curcumin; and complexation with milk protein enhances solubility, adsorption, and retention in systemic circulation. Our study brings out molecular-level insights into how the co-administration of Piperine with Curcumin facilitates the formation of a stable molecular complex, which in turn enhances the bioavailability of Curcumin through its favourable interactions with milk proteins. These findings offer a theoretical understanding for the improved therapeutic efficacy observed in traditional Siddha formulations, highlighting the potential of such synergistic

combinations in the development of effective drug formulations.

In future studies, experimental validations can be carried out to substantiate the computational findings. Techniques such as fluorescence quenching, circular dichroism (CD) spectroscopy, and Fourier-transform infrared (FTIR) spectroscopy may be employed to characterize binding interactions between Curcumin, Piperine, and milk proteins. *In-vitro* assay studies will bridge the gap between theoretical predictions and practical therapeutic applications, thereby strengthening the translational potential of this work.

CRediT authorship contribution statement

Madhesh Palanisamy: Writing – review & editing, Writing – original draft, Methodology, Investigation, Formal analysis, Data curation, Conceptualization. **Vidya Ravindran:** Writing – review & editing, Supervision, Software, Resources, Project administration, Methodology, Investigation, Conceptualization. **Gayathri Krishnamoorthy:** Writing – original draft, Methodology, Investigation, Conceptualization.

Declaration of Competing Interest

The authors declare no potential conflicts of interest.

Acknowledgement

The authors would like to thank the financial support provided by the Centre for Research, Anna University, India, through Anna Research Fellowship (ARF), and Department of Science and Technology—Science and Engineering Research Board (DST-SERB), India, through the project "Engineering Two-dimensional Nanostructure for Drug–carrier Applications" under Core Research Grant. Project Number: CRG/2020/006330.

Appendix A. Supporting information

Supplementary data associated with this article can be found in the online version at doi:10.1016/j.compbiolchem.2025.108672.

References

- Ali, I.S., Kishwar, W., Diana, H., 2013. Synthesis, DNA binding, hemolytic, and anticancer assays of curcumin-based ligands and their ruthenium(III) complexes. Med. Chem. Res. 22, 1386–1398.
- Arivazhagan, M., et al., 2015. Vibrational spectroscopic (FTIR and FT-Raman), first-order hyperpolarizability, HOMO, LUMO, NBO, mulliken charge analyses of 2-ethylimidazole based on Hartree–Fock and DFT calculations. Spectrochim. Acta Part A Mol. Biomol. Spectrosc. 134, 493–501.
- Benchmarking Antioxidant-Related Properties for Gallic Acid through the Use of DFT, 2021. MP2, CCSD, and CCSD(T) approaches. Gabriel L. C. De. Souza Kirk. A. Peterson J. Phys. Chem. A 125 (1), 198–208. https://doi.org/10.1021/acs.jpca.0c09116.
- Berman, H.M., Westbrook, J., Feng, Z., Gilliland, G., Bhat, T.N., Weissig, H., Shindyalov, I.N., 2000. P.E. Bourne, the protein data bank. Nucleic Acids Res. 28, 235–242. https://doi.org/10.1093/nar/28.1.235.
- Boulmokh, Y., Belguidoum, K., Meddour, F., et al., 2023. Enhanced antioxidant properties of novel curcumin derivatives: a comprehensive DFT computational study. Struct. Chem. https://doi.org/10.1007/s11224-023-02237-6.
- Bronze-Uhle, E.S., Costa, B.C., Ximenes, V.F., Lisboa-Filho, P.N., 2017. Synthetic nanoparticles of bovine serum albumin with entrapped salicylic acid. Nanotechnol. Sci. Appl. 10, 11.
- Bujacz, A., 2012. Structures of bovine, equine and leporine serum albumin. Acta Crystallogr. Sect. D. Biol. Crystallogr. 68 (10), 1278–1289. https://doi.org/10.1107/ S0907444912027047.
- Changeux, J.-P., 2013. The concept of allosteric modulation: an overview. Drug Discov. Today. Technol. 10, e223–e228.
- Chrysina, E.D., Brew, K., Acharya, K.R., 2000. Crystal structures of Apo- and holo-bovine α-lactalbumin at 2.2-Å resolution reveal an effect of calcium on inter-lobe interactions. J. Biol. Chem. 275 (47), 37021–37029. https://doi.org/10.1074/jbc. M004752200.
- Davoodi, S.H., et al., 2016. Health-related aspects of milk proteins," *iran.* J. Pharm. Res. 15 (3), 573–591.
- Esatbeyoglu, T., Huebbe, P., Insa, M.A., DawnChin, E., Wagner, A.E., Rimbach, G., 2012. Curcumin—From molecule to biological function. Angew. Chem. Int. Ed. 51, 5308–5332.

- Ganji, M.D., 2015. Graphene: a first-principles B3LYP-D3 study, 2, 2504–2511. https://doi.org/10.1039/c4cr004399e
- Gaussian 16, Revision C.01, M.J. Frisch, G.W. Trucks, H.B. Schlegel, G.E. Scuseria, M.A. Robb, J.R. Cheeseman, G. Scalmani, V. Barone, G.A. Petersson, H. Nakatsuji, X. Li, M. Caricato, A.V. Marenich, J. Bloino, B.G. Janesko, R. Gomperts, B. Mennucci, H.P. Hratchian, J.V. Ortiz, A.F. Izmaylov, J.L. Sonnenberg, D. Williams-Young, F. Ding, F. Lipparini, F. Egidi, J. Goings, B. Peng, A. Petrone, T. Henderson, D. Ranasinghe, V.G. Zakrzewski, J. Gao, N. Rega, G. Zheng, W. Liang, M. Hada, M. Ehara, K. Toyota, R. Fukuda, J. Hasegawa, M. Ishida, T. Nakajima, Y. Honda, O. Kitao, H. Nakai, T. Vreven, K. Throssell, J.A. Montgomery, Jr, J.E. Peralta, F. Ogliaro, M.J. Bearpark, J. J. Heyd, E.N. Brothers, K.N. Kudin, V.N. Staroverov, T.A. Keith, R. Kobayashi, J. Normand, K. Raghavachari, A.P. Rendell, J.C. Burant, S.S. Iyengar, J. Tomasi, M. Cossi, J.M. Millam, M. Klene, C. Adamo, R. Cammi, J.W. Ochterski, R.L. Martin, K. Morokuma, O. Farkas, J.B. Foresman, and D.J. Fox, Gaussian, Inc., Wallingford C.T., 2016.
- GaussView, Version 6.1, 2016. Roy dennington, todd A. Keith, and john M. Millam, semichem inc., shawnee mission. KS.
- Grykiewicz, G., Silfirski, P., 2012a. Curcumin and curcuminoids in the quest for medicinal status. Acta Biochim. Pol. 59, 201–212.
- Grykiewicz, G., Silfirski, P., 2012b. Curcumin and curcuminoids in the quest for medicinal status. Acta Biochim. Pol. 59, 201–212.
- Gupta, S., Prasad, S., Ji, H.K., Patchva, S., Webb, L.J., Priyadarsini, K.I., Aggarwal, B.B., 2011. Multitargeting by curcumin as revealed by molecular interaction studies. Nat. Prod. Rep. 28, 1937–1955.
- Haug, A., Høstmark, A.T., Harstad, O.M., 2007. Bovine milk in human nutrition a review. Lipids Health Dis. 6, 1–16. https://doi.org/10.1186/1476-511X-6-25.
- He, Jixiao, Liu, Xinyi, Zhu, Chunhao, et al., January 2024. ASD2023: towards the integration of landscapes of allosteric knowledgebase. Nucleic Acids Res. Nucleic Acids Res. 52 (D1), D376–D383. https://doi.org/10.1093/nar/gkad915.
- Humphrey, William, et al., 1996. "VMD: visual molecular dynamics. J. Mol. Graph. 14 (1), 33–38. https://doi.org/10.1016/0263-7855(96)00018-5.
- Javed, S., Kohli, K., Ahsan, W., 2007. An in vivo pharmacokinetic study. Bioavailab. Augment. silvmarin Using Nat. bioenhancers 1–11.
- Jeliński, T., Przybyłek, M., Cysewski, P., 2019. Natural deep eutectic solvents as agents for improving solubility, stability and delivery of curcumin. Pharm. Res. 36, 116. https://doi.org/10.1007/s11095-019-2643-2.
- Khajuria, A., Thusu, N., Zutshi, U., 2002. Piperine modulates permeability characteristics of the intestine by inducing alterations in membrane dynamics: influence on brush border membrane fluidity, ultrastructure, and enzyme kinetics. Phytomedicine 9 (3), 224-231.
- Kolev, Tsonko M., et al., 2005. "DFT and experimental studies of the structure and vibrational spectra of curcumin. Int. J. Quantum Chem. 102 (6), 1069–1079.
- Kumar, V., Lewis, S.A., Mutalik, S., Shenoy, D.B., Venkatesh, Udupa, N., 2002 Apr. Biodegradable microspheres of curcumin for the treatment of inflammation. Indian J. Physiol. Pharmacol. 46 (2), 209–217. PMID: 12500496.
- J. Physiol. Pharmacol. 46 (2), 209–217. PMID: 12500496. Kuttan, R., Sudheeran, P.C., 1987. And joseph, C.D. Turmeric and curcumin as topical agents in cancer therapy. Tumori 73 (1), 29–31.
- Kuttan, R., Bhanumathy, P., Nirmala, K., George, M.C., 1985. Potential anticancer activity of turmeric (Curcuma longa). Cancer Lett. 29 (2), 197–202.
- Liu, J., Nussinov, R., 2016. Allostery: an overview of its history, concepts, methods, and applications. PLoS Comput. Biol. 12, e1004966 (No).
- Loch, J., et al., 2011. Two modes of fatty acid binding to bovine β-lactoglobulincrystallographic and spectroscopic studies. J. Mol. Recognit. 24 (2), 341–349. https://doi.org/10.1002/imr. 1084.
- Lu, Feng, Cheng, Xianhui, Qi, Xiulei, Li, Dejun, Hu, Lianghai, 2025. Metabolic landscaping of extracellular vesicles from body fluids by phosphatidylserine imprinted polymer enrichment and mass spectrometry analysis. Talanta 282, 126940. https://doi.org/10.1016/j.talanta.2024.126940.
- Lu, T., Chen, F., 2012. Multiwfn: a multifunctional wavefunction analyzer. J. Comput. Chem. 33 (5), 580–592. https://doi.org/10.1002/jcc.22885.
- McSweeney, P.L.H., Fox, P.F., 2009. Adv. Dairy Chem. 3. https://doi.org/10.1007/978-0-387-84865-5.
- Mohan, R., Sivak, J., Ashton, P., Russo, L.A., Pham, B.Q., Kasahara, N., Raizman, M.B., Fini, M.E., 2000. Curcuminoids inhibit the angiogenic response stimulated by fibroblast growth factor-2, including expression of matrix metalloproteinase gelatinase b. J. Biol. Chem. 275 (14), 10405–10412.
- Mulliken, Robert S., 1939. "Intensities of electronic transitions in molecular spectra II. Charge-transfer Spectra. J. Chem. Phys. 7 (1), 20–34.
- Otero-de-la-Roza, Alberto and Johnson, Erin R. and Contreras-García, Julia, "Revealing non-covalent interactions in solids: NCI plots revisited", "Phys. Chem. Chem. Phys." 20122, volume 14/35, 12165-12172, The Royal Society of Chemistry, 10.1039/ C2CP4139
- Ouaket, A., Chraka, A., Raissouni, I., Amrani, M.A.E., Berrada, M., Knouzi, N., 2022. Synthesis, spectroscopic (13C/¹H NMR, FT-IR) investigations, quantum chemical modelling (FMO, MEP, NBO analysis), and antioxidant activity of the bisbenzimidazole molecule. J. Mol. Struct. 1259, 132729. https://doi.org/10.1016/j molstruc.2022.132729.
- Pan, M.H., Huang, T.M., Lin, J.K., 1999 Apr. Biotransformation of curcumin through reduction and glucuronidation in mice. Drug Metab. Dispos. 27 (4), 486–494. PMID: 10101144.
- Pettersen, Eric F., et al., 2004. "UCSF Chimera—A visualization system for exploratory research and analysis. J. Comput. Chem. 25 (13), 1605–1612. https://doi.org/ 10.1002/jcc.20084.
- Prasad, S., Aggarwal, B.B., 2011. Turmeric, the golden spice: from traditional Medicine to modern Medicine. In: Benzie, I.F.F., Wachtel-Galor, S. (Eds.), Herbal Medicine: Biomolecular and Clinical Aspects. 2nd edition. Boca Raton (FL): CRC Press/Taylor

- & Francis. Chapter 13. Available from: \(\lambda \text{https://www.ncbi.nlm.nih.gov/books/NB} \)
- Priyadarsini, K.I., 2013. Chemical and structural features influencing the biological activity of curcumin. Curr. Pharm. Des. 19, 2093–2100.
- Priyadarsini, K.I., 2014b. The chemistry of curcumin: from extraction to therapeutic agent. Molecules 19, 20091–20112. https://doi.org/10.3390/molecules191220091.
- Priyadarsini, K.I., 2014a. The chemistry of curcumin: from extraction to therapeutic agent. Molecules 19, 20091–20112. https://doi.org/10.3390/molecules191220091.
- Raghunath, I., Koland, M., Narayanan, A.V., 2024. Piperine: a possible permeation enhancer for oral protein delivery. J. Appl. Pharm. Sci. 14 (04), 035–045. https:// doi.org/10.7324/JAPS.2024.157160.
- Sharifi-Rad, J., Rayess, Y.E., Rizk, A.A., Sadaka, C., Zgheib, R., Zam, W., et al., 2020. Turmeric and its major compound curcumin on health: bioactive effects and safety profiles for food, pharmaceutical, biotechnological and medicinal applications. Front. Pharmacol. 11, 1021. https://doi.org/10.3389/fphar, 2020.01021.
- Sharma, R.A., Gescher, A.J., Steward, W.P., 2005. Curcumin: the story so far. ISSN 0959-8049 Eur. J. Cancer 41 (13), 1955–1968. https://doi.org/10.1016/j.
- Shoba, G., Joy, D., Joseph, T., Majeed, M., Rajendran, R., Srinivas, P.S., 1998 May. Influence of piperine on the pharmacokinetics of curcumin in animals and human volunteers. Planta Med. 64 (4), 353–356. https://doi.org/10.1055/s-2006-957450. PMID: 9619120

- Siviero, Angelo, Gallo, Eugenia, Maggini, Valentina, Gori, Luigi, Mugelli, Alessandro, Firenzuoli, Fabio, Vannacci, Alfredo, 2015. Curcumin, a golden spice with low bioavailability. ISSN 2210-8033 J. Herb. Med. 5 (2), 57–70. https://doi.org/10.1016/j.hermed.2015.03.001.
- Solanki, Raghu, Rostamabadi, Hadis, Patel, Sunita, Jafari, Seid Mahdi, 2021. Anticancer nano-delivery systems based on bovine serum albumin nanoparticles: a critical review. ISSN 0141-8130 Int. J. Biol. Macromol. 193, 528–540. https://doi.org/ 10.1016/j.ijbiomac.2021.10.040.
- Soleimani, V., Sahebkar, A., Hosseinzadeh, H., 2018. Turmeric (Curcuma longa) and its major constituent (Curcumin) as nontoxic and safe substances: review. Phytother. Res. 32 (6), 985–995. https://doi.org/10.1002/ptr.6054.
- Solution Conformations of Curcumin in DMSO Cathryn, Slabber, A., Craig, D., Grimmer, Ross, S., 2016. Robinson J. Nat. Prod. 79 (10), 2726–2730. https://doi.org/10.1021/ acs.jnatprod.6b00726.
- Song, K., Liu, X., Huang, W., Lu, S., Shen, Q., Zhang, L., Zhang, J.*, 2017. Improved method for the identification and validation of allosteric sites. J. Chem. Inf. Model. https://doi.org/10.1021/acs.jcim.7b00014.
- Trott, O., Olson, A.J., 2010. AutoDock vina: improving the speed and accuracy of docking with a new scoring function, efficient optimization, and multithreading. J. Comput. Chem. 31 (2), 455–461. https://doi.org/10.1002/jcc.21334.
- Yang, Z., Zhang, N., Ma, T., Liu, L., Zhao, L., Xie, H., 2020. Engineered bovine serum albumin-based nanoparticles with pH-sensitivity for doxorubicin delivery and controlled release. Drug Deliv. 27 (1), 1156–1164.